Eur. Phys. J. A **29**, 209–220 (2006)
DOI 10.1140/epja/i2006-10070-4

THE EUROPEAN PHYSICAL JOURNAL A

ϕ-meson photoproduction from nuclei

A. Sibirtsev[1,a], H.-W. Hammer[1], U.-G. Meißner[1,2], and A.W. Thomas[3]

[1] Helmholtz-Institut für Strahlen- und Kernphysik (Theorie), Universität Bonn, Nußallee 14-16, D-53115 Bonn, Germany
[2] Institut für Kernphysik (Theorie), Forschungszentrum Jülich, D-52425 Jülich, Germany
[3] Jefferson Lab, 12000 Jefferson Ave., Newport News, VA 23606, USA

Received: 22 June 2006 /
Published online: 25 July 2006 –
Communicated by Th. Walcher

Abstract. We study coherent and incoherent ϕ-meson photoproduction from nuclei. The available data are analyzed in terms of single- and coupled-channel photoproduction. It is found that the data on coherent photoproduction can be well reproduced within a single-channel optical model and show only little room for ω-ϕ mixing. These data indicate a normal distortion of the ϕ-meson in nuclei, which is compatible with the results obtained through the vector meson dominance model. The data on incoherent ϕ-meson photoproduction show an anomalous A-dependence resulting in a very strong ϕ-meson distortion. These data can be explained by a coupled-channel effect through the dominant contribution from the $\omega \to \phi$ or the $\pi \to \phi$ transition or, more speculative, through the excitation of a cryptoexotic B_ϕ-baryon.

PACS. 11.80.Gw Multichannel scattering – 12.40.Vv Vector-meson dominance – 13.60.-r Photon and charged-lepton interactions with hadrons – 25.20.Lj Photoproduction reactions

1 Introduction

The renormalization of the meson spectral function in nuclear matter (for some early references, see [1–6] and a recent review is [7]) attracted substantial interest in connection with the measurements of the di-lepton invariant mass spectra from heavy-ion collisions [8–10]. Recently, experimental results on ω- and ϕ-meson modification at normal nuclear densities have been reported in experiments involving photon and proton beams [11–16]. The most remarkable result obtained in all these experiments is the anomalous A-dependence of the ϕ-meson production from nuclear targets. At the same time the A-dependence of the ω-meson production both in γA and pA interactions can be well understood.

At the threshold of elementary ϕ-meson production, its momentum in the laboratory system, *i.e.* with respect to nuclear matter, is quite high and a substantial fraction of the ϕ-mesons decay outside the nucleus. Only that small fraction which decays inside the nucleus would indicate a probable pole shift of the spectral function. Therefore one could not expect to observe a significant in-medium modification of the ϕ-meson mass by measuring the dileptonic or K^+K^- invariant mass spectra. However, it is very plausible to study the modification of the ϕ-meson width, since at low densities it is related to the imaginary part of the forward ϕN scattering amplitude [17–19]. The latter determines the ϕ-meson distortion in the nucleus, which can be studied by measuring the A-dependence of the ϕ-meson production.

Such ideas motivated experiments on ϕ-meson production from nuclei at the KEK-PS [15], SPRING-8 [20] and at COSY [21]. Here we analyze recent results on incoherent ϕ-meson photoproduction from nuclei collected at SPRING-8 [20], which indicate a substantial distortion of the ϕ-meson in finite nuclei. For consistency, we also analyze data on coherent ϕ-meson photoproduction collected at Cornell some time ago [22]. We investigate the role of single- and coupled-channel effects in ϕ-meson photoproduction and provide a possible explanation of the observed anomaly.

The manuscript is organized as follows. In sect. 2, we analyze the elementary amplitudes $\gamma p \to \phi p$ and $\gamma p \to \omega p$ in terms of the vector meson dominance model and compare to data taken at Cornell, ELSA and SPRING-8. In sect. 3, we study coherent and incoherent ϕ-meson photoproduction off nuclear targets in a single-channel optical model and show that such an approach is not capable of describing the new data from SPRING-8. The coupled-channel scattering is considered in sect. 4 and it is in particular shown that the A-dependence of the SPRING-8 data can be understood in a two-step model, including ω-ϕ mixing and coupling to an intermediate pion. We also add some speculations about the excitation of crypto-exotuic baryons with hidden strangeness. Section 5 contains our conclusions.

[a] e-mail: a.sibirtsev@fz-juelich.de

2 The vector dominance model

2.1 Data evaluation

Considering quark–anti-quark fluctuations of the photon, the Vector Dominance Model (VDM) assumes that intermediate hadronic $q\bar{q}$ states are entirely dominated by the neutral vector mesons. In that sense the hadron-like photon [23] is a superposition of all possible vector meson states. The $\gamma N \to \phi N$ reaction can be decomposed into the transition of the photon to a virtual vector meson V followed by the elastic or inelastic vector meson scattering on the target nucleon. The invariant reaction amplitude follows as [24,25]

$$\mathcal{M}_{\gamma N\to\phi N} = \sum_V \frac{\sqrt{\pi\alpha}}{\gamma_V}\mathcal{M}_{VN\to\phi N}, \tag{1}$$

where the summation is performed over vector meson states, α is the fine structure constant, γ_V is the photon coupling to the vector meson V and $\mathcal{M}_{VN\to\phi N}$ is the amplitude for the $VN \to \phi N$ transition.

A direct determination of γ_V is possible through vector meson decay into a lepton pair [26]

$$\Gamma(V \to l^+l^-) = \frac{\pi\alpha^2}{3\gamma_V^2}\sqrt{m_V^2 - 4m_l^2}\left[1 + \frac{2m_l^2}{m_V^2}\right], \tag{2}$$

where m_V and m_l are the masses of vector meson and lepton, respectively. Taking the di-electron decay width from ref. [27], the photon coupling to the lightest vector mesons is given as

$$\gamma_\rho \div \gamma_\omega \div \gamma_\phi = 2.48 \div 8.53 \div 6.69. \tag{3}$$

Although the couplings γ_V can be determined experimentally, eq. (1) does not indicate whether non-diagonal, *i.e.* $\rho N \to \phi N$ and $\omega N \to \phi N$, or diagonal $\phi N \to \phi N$ processes dominate the ϕ-meson photoproduction on the nucleon, since the $\mathcal{M}_{V\phi}$ amplitudes cannot be measured. Furthermore, VDM suggests that the virtual vector meson stemming from the photon becomes real through the four-momentum t transferred to the nucleon, which in general requires the introduction of a form factor in the interaction vertices [28–30].

The next step in the VDM analysis is to consider only the diagonal transition or elastic $VN \to VN$ scattering. The imaginary part of the amplitude $f^*_{\phi N}(0)$ in the center of mass for forward elastic $\phi N \to \phi N$ scattering is related to the ϕN total cross-section, $\sigma_{\phi N}$, by an optical theorem as[1]

$$\Im f^*_{\phi N\to\phi N}(q_\phi, \theta = 0) = \frac{q_\phi}{4\pi}\,\sigma_{\phi N}, \tag{4}$$

where q_ϕ and θ are the ϕ-meson momentum and scattering angle in the ϕN center-of-mass system, respectively. The amplitude $f^*_{\phi N}$ is related to the Lorentz invariant scattering amplitude as

$$\mathcal{M}_{\phi N\to\phi N} = -8\pi\ \sqrt{s}\ f^*_{\phi N\to\phi N}(q_\phi, \theta), \tag{5}$$

with s the invariant collision energy squared. The $\gamma N \to \phi N$ differential cross-section is given in terms of the Lorentz invariant amplitude as

$$\frac{\mathrm{d}\sigma_{\gamma N\to\phi N}}{\mathrm{d}t} = \frac{|\mathcal{M}_{\gamma N\to\phi N}|^2}{64\pi s q_\gamma^2}, \tag{6}$$

where q_γ is the photon momentum in the center-of-mass system. By introducing the ratio of the real to the imaginary part of the forward ϕN scattering amplitude as α_ϕ, the $\gamma N \to \phi N$ differential cross-section at $t = 0$ can be written as[2]

$$\left.\frac{\mathrm{d}\sigma_{\gamma N\to\phi N}}{\mathrm{d}t}\right|_{t=0} = \frac{\alpha}{16\gamma_\phi^2}\,\frac{q_\phi^2}{q_\gamma^2}\,(1+\alpha_\phi^2)\,\sigma_{\phi N}^2. \tag{7}$$

Again, both the ratio α_ϕ and the total ϕN cross-section are unknown. Thus, the VDM analysis of photoproduction data requires additional assumptions.

It is believed that at high energies the hadronic forward scattering amplitudes are purely imaginary. The data available [27] for the pp, $\bar{p}p$, π^-p, π^+p, K^+p and K^-p reactions indicate that the ratios of the real to imaginary parts of the forward scattering amplitudes are $\simeq 0.1$ at $\sqrt{s} > 20$ GeV. The α_ϕ ratio was measured [31] through the interference between the $\phi \to e^+e^-$ decay and the Bethe-Heitler production of electron-positron pairs and it was found that $\alpha_\phi = -0.48^{+0.33}_{-0.45}$ at photon energies $6 < E_\gamma < 7.4$ GeV. This result is too uncertain to be used in the further analysis. To estimate the maximum value of $\sigma_{\phi N}$, we apply $\alpha_\phi = 0$. It is clear that any non-vanishing ratio α_ϕ would result in a reduction of the ϕN cross-section that will be evaluated from the data in what follows.

Now fig. 1 shows the available data [32–41] on the forward $\gamma p \to \phi p$ differential cross-section as a function of the photon energy. The lines are the results using eq. (7) obtained with $\alpha_\phi = 0$ and for different values of the total ϕN cross-section. Only one experimental point at high energy [39] needs a large $\sigma_{\phi N}$, although within experimental uncertainty this measurement is in agreement with the data at photon energies below 10 GeV, which are also shown in fig. 2. Note that a large part of the data shown in fig. 2 is in reasonable agreement with calculations done with $\sigma_{\phi N} \simeq 11$ mb.

Figure 2 demonstrates the disagreement between the most recent measurements from SAPHIR [40] and SPRING-8 [41], which are shown by the solid circles and the solid triangles, respectively. Note that both sets of

[1] It is clear that this formalism holds for the photoproduction of any vector meson $V = \rho, \omega, \phi, J/\Psi, \ldots$.

[2] Note that the q_V^2/q_γ^2 ratio was not included in most of the VDM analyses reviewed in ref. [24]. While this simplification might be applicable at high energies, that is not the case for most of the data available at $E_\gamma < 10$ GeV, as is illustrated by fig. 2.

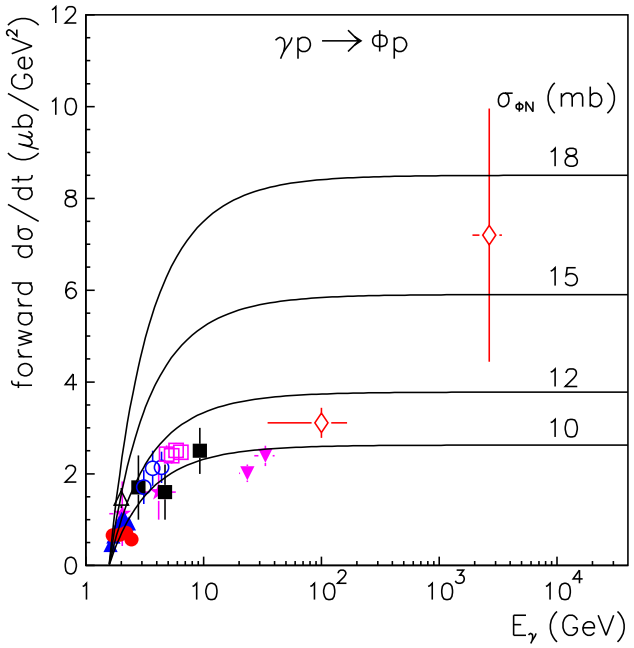

Fig. 1. The forward $\gamma p \to \phi p$ differential cross-section as a function of photon energy. The data are taken from refs. [32–41]. The lines show the calculations using eq. (7) with $\alpha_\phi = 0$ and for different values of $\sigma_{\phi N}$.

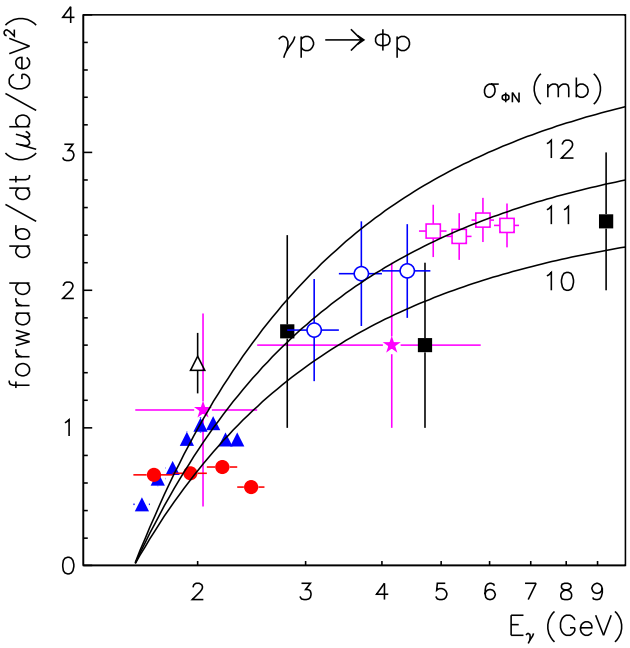

Fig. 2. Same as in fig. 1 for a low photon energy scale. The solid circles show the results collected by SAPHIR [40], while the solid triangles are the measurements from SPRING-8 [41].

data contradict the VDM predictions. Although this discrepancy requires special investigation we would like to make the following comments relevant to the present study and VDM analysis of the data.

2.2 Comments

Let us discuss the observed discrepancy between the data and the VDM description at low energies through inspection of the forward $\gamma p \to \omega p$ differential cross-section, shown in fig. 3 as a function of the photon energy. The different symbols indicate the data collected in ref. [42], while the solid lines show the VMD calculations based on eq. (7) with the ratio $\alpha_\omega = 0$ and for different values of $\sigma_{\omega N}$, respectively. The data at $E_\gamma > 10$ GeV are in good agreement with the VDM assuming that $20 < \sigma_{\omega N} < 30$ mb. The low-energy $\gamma p \to \omega p$ data indicate an excess with respect to VDM that is well understood in terms of the non-diagonal $\rho N \to \omega N$ transition given by eq. (1). More precisely, this can be explained by a π-meson exchange contribution [24,43]. Indeed, the dominant ω-meson decay mode is $\pi^+\pi^-\pi^0$, which in general is described in terms of the transition $\omega \to \rho\pi$, followed by the $\rho \to \pi\pi$ decay. Therefore it is natural to expect that the non-diagonal $\rho N \to \omega N$ transition plays a substantial role in (low-energy) ω-meson photoproduction.

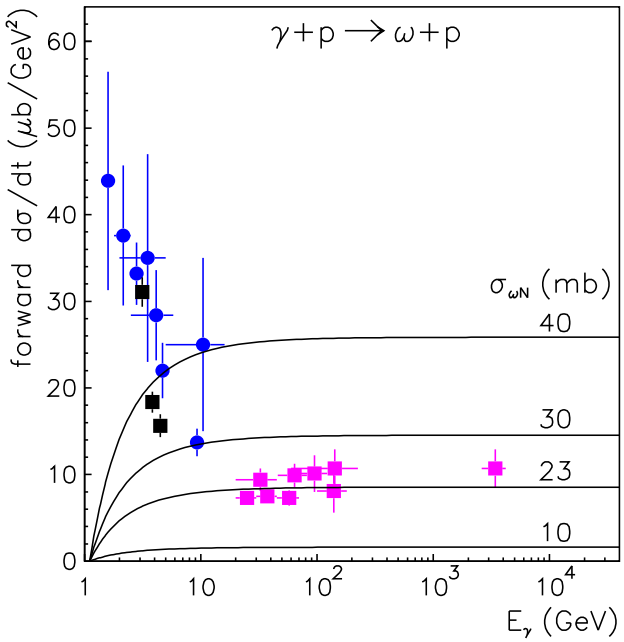

Fig. 3. The forward $\gamma p \to \omega p$ differential cross-section as a function of photon energy. The data are collected in ref. [42]. The lines show the calculations based on eq. (7) with $\alpha_\omega = 0$ and for different values of $\sigma_{\omega N}$.

Most of the results on the forward photoproduction cross-section are determined through an extrapolation of the differential $d\sigma/dt$ cross-section over a certain range of t, not to the maximal accesible value, but rather to the point $t = 0$, by applying a fit of the form $d\sigma/dt = A\exp(bt)$. This is the reason why the $t = 0$ differential cross-sections at low photon energies, shown in fig. 3, do not vanish even though they are clearly dominated by π-meson exchange. The extrapolation to different t might explain the difference between the SAPHIR [40]

and SPRING-8 [41] results and data available at higher energies.

Indeed, within the Born approximation the π-meson exchange contribution vanishes [42–45] at $t = 0$. Here the minimal and maximal value of t is given by

$$t^{\pm} = m_V^2 - \frac{s - m_N^2}{2s}\left(s + m_V^2 - m_N^2 \mp \left[(s - m_V^2 - m_N^2)^2 - 4m_V^2 m_N^2\right]^{1/2}\right), \quad (8)$$

with m_V and m_N the masses of the vector meson and nucleon, respectively. At threshold, $\sqrt{s} = m_V + m_N$, the four-momentum transfer squared is

$$t^{\pm} = -\frac{m_N\, m_V^2}{m_N + m_V}, \quad (9)$$

with increasing energy, $\sqrt{s} \gg m_V + m_N$,

$$t^{-} \simeq m_V^2 - \frac{(s - m_N^2)\, m_V^2}{s}, \quad (10)$$

and t^- approaches zero.

It is not obvious whether the extrapolation should be done to $t = 0$ or to $\theta = 0$, as is explicitly shown by eq. (4). Note that for elastic scattering $t^- = 0$. Actually the differential $\gamma p \to \phi p$ cross-sections measured by SAPHIR [40] and SPRING-8 [41] shown in fig. 2 were extrapolated to $t = t^-$ and the $t = 0$ correction in that case is $\exp(-t^-)$, which accounts for a factor $\simeq 1.61$ at the ϕ-meson photoproduction threshold.

Keeping that in mind one might conclude that similar to the $\gamma p \to \omega p$ data the forward $\gamma p \to \phi p$ differential cross-section indicates some enhancement with respect to the diagonal VDM. This enhancement might stem from non-diagonal transitions[3]. Apparently that problem requires additional investigation, which is beyond the scope of the current study.

Moreover, the discrepancy between the SAPHIR [40] and SPRING-8 [41] results can be partially explained by the different range of t used for the $t = t^-$ extrapolation. SPRING-8 explored the range $t - t^- > 0.4$ GeV^2, while the SAPHIR measurements were used to fit $\mathrm{d}\sigma/\mathrm{d}t$ over a larger range and at maximum photon energy $t - t^- > -2$ GeV^2. For that reason it is worthwhile to re-analyze the SAPHIR data by fitting the differential cross-section with the sum of a soft and a hard component.

Finally, keeping in mind the uncertainty of the analysis of low-energy data on the forward $\gamma p \to \phi p$ differential cross-section we conclude that VDM yields the upper limit of the total ϕp cross-section about 11 mb. If the ratio of the real to imaginary forward scattering amplitude, *i.e.* α_ϕ, is not equal to zero, then $\sigma_{\phi p}$ can be even smaller, as indicated by eq. (7).

[3] Both SAPHIR and SPRING-8 measurements of angular spectra in the Gottfried-Jackson frame support this conclusion.

3 Single-channel optical model

Consider a nuclear reaction as a succession of collisions of the incident particle with individual nucleons of the target. If the nucleus is sufficiently large the reaction can be formulated in terms of the optical model through replacement of the multiple individual interactions by an effective potential interaction with nuclear matter. Within the so-called $t\rho$ approximation, that is valid at normal nuclear densities, $\rho = 0.16$ fm^{-3}, the optical potential is given by the product of the density and forward two-body scattering amplitude. Similarly, the Glauber theory expresses the cross-section for reactions on nuclear target in terms of elementary two-body interactions [46–48].

Conversely, by measuring the nuclear cross-sections it might be possible to study the elementary interactions [24]. The realization of Drell and Trefil [49] and Margolis [50] that such a formalism could be used to study the interaction of unstable particles with the nucleon by producing them in a nucleus with hadronic or electromagnetic beams, stimulated enormous experimental activity [24]. This method was first applied [49–51] for the evaluation of the ρN interaction from coherent and incoherent ρ-meson photoproduction off nuclei. Coherent photoproduction has the advantage that the produced particle must have quantum numbers similar to those of the photon.

3.1 Coherent photoproduction

An extensive study of coherent ϕ-meson photoproduction on a variety of nuclear targets was done at the Cornell 10 GeV electron synchrotron [22]. One might expect [50, 51] the A-dependence of coherent photoproduction at high energies to be proportional to A^2 if the ϕ-meson does not interact in nuclei, *i.e.* if it is not distorted by final-state interactions (FSI). By fitting the forward ϕ-meson photoproduction cross-section [22] with a function $\sim A^\alpha$, one obtains the slope $\alpha = 1.37 \pm 0.08$ at the photon energy of 6.4 GeV and $\alpha = 1.53 \pm 0.05$ at $E_\gamma = 8.3$ GeV. The shaded boxes in fig. 4 show these results, which indicate a strong deviation from a dependence on A^2.

Note, however, that the forward photoproduction cross-section contains both coherent and incoherent contributions. In the absence of the FSI distortion, the incoherent photoproduction cross-section is proportional to A. Therefore one might argue that the A-dependence results from a mixture of coherent and incoherent ϕ-meson photoproduction. In order to verify such a possibility, an additional experiment with linearly polarized photons with average energy of 5.7 GeV was performed [52]. The measured polarization asymmetry for the forward ϕ-meson photoproduction from a carbon target was found to be consistent with the assumption of coherent photoproduction[4].

[4] At the same time the asymmetry from the hydrogen target seems to be inconsistent with purely elastic ϕ-meson photoproduction. As we discussed in sect. 2, this Cornell observation [52] is in agreement with the most recent results from SAPHIR [40] and SPRING-8 [41].

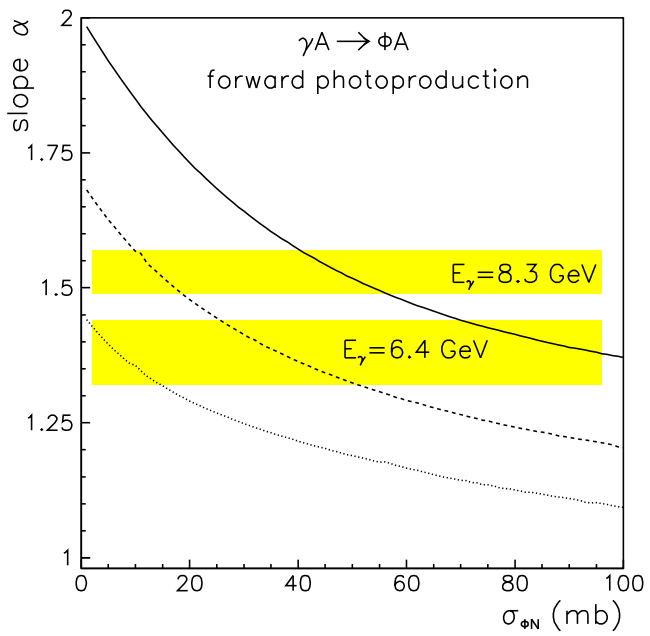

Fig. 4. The slope α of the A^{α}-dependence of the forward ϕ-meson photoproduction cross-section as a function of the total ϕN cross-section. The shaded boxes indicate the results at photon energies 6.4 and 8.3 GeV obtained at Cornell [22]. The lines show the calculations by eq. (14) with different longitudinal momenta $q_l = 0$ (solid), 63 (dashed) and 82 MeV/c (dotted), which are fixed to the photon energy by eq. (12). The calculations were done for the ratio $\alpha_\phi = 0$.

In order to evaluate the ϕN interaction from coherent photoproduction one can apply the method proposed in refs. [50,51] and express the amplitude for coherent ϕ-meson photoproduction from nuclei as [24,49,51,53–55]

$$\mathcal{T}^{coh}_{\gamma A\to\phi A}(t,A) = \mathcal{T}_{\gamma N\to\phi N}\int\limits_0^\infty \mathrm{d}^2b\, J_0(q_t\, b) \times \int\limits_{-\infty}^{\infty} \mathrm{d}z\, \rho(b,z) \exp\left[iq_l z\right] \left[1 - i\chi_\phi(b,z)\right]^{A-1}, \qquad (11)$$

where $\mathcal{T}_{\gamma N}$ is the elementary photoproduction amplitude on a nucleon, an integration is performed over the impact parameter b, the z coordinate is along the beam direction and $\rho(r = \sqrt{b^2+z^2})$ is the nuclear density function normalized to the number of the nucleons in the nucleus. Here, t is the four-momentum transferred to the nucleus and $-t = q_l^2 + q_t^2$, with q_l and q_t being the longitudinal and transverse component, respectively, given by

$$q_l = k - \cos\theta\sqrt{k^2 - m_\phi^2}, \qquad q_t = \sin\theta\sqrt{k^2 - m_\phi^2}, \qquad (12)$$

where k is the photon momentum, m_ϕ is the pole mass of the ϕ-meson and θ is the emission angle of the produced ϕ-meson. In eq. (11) J_0 is the zero-order Bessel function. The last term of eq. (11) accounts for the distortion of the ϕ-meson through an effective interaction with A–1 nuclear nucleons and χ_ϕ is the corresponding nuclear phase shift. Here we neglect the distortion of the photon. The phase shift χ_ϕ can be well approximated within the impulse approximation by [56,57]

$$\chi_\phi(b,z) = -\frac{2\pi\, f_{\phi N}(p_\phi, \theta = 0)}{p_\phi}\int\limits_z^\infty \rho(b,y)\mathrm{d}y, \qquad (13)$$

where $f_{\phi N}$ is the complex amplitude for the forward ϕN elastic scattering taken now in the rest frame with respect to the nucleus, *i.e.* in the laboratory system. Note that p_ϕ is the ϕ-meson momentum in the laboratory frame. The imaginary part of the $f_{\phi N}$ amplitude is related through the optical theorem to the total cross-section $\sigma_{\phi N}$, similar to eq. (4), replacing q_ϕ by p_ϕ.

By introducing the ratio of the real to imaginary part of the forward ϕN scattering amplitude, α_ϕ, the cross-section for coherent ϕ-meson photoproduction from nuclei is finally given as

$$\frac{\mathrm{d}\sigma^{coh}_{\gamma A\to\phi A}}{\mathrm{d}t} = \frac{\mathrm{d}\sigma_{\gamma N\to\phi N}}{\mathrm{d}t}\left|\int\limits_0^\infty \mathrm{d}^2b\, J_0(q_t b)\int\limits_{-\infty}^{\infty}\mathrm{d}z\,\rho(b,z) \times \exp\left[iq_l z\right]\exp\left[\frac{\sigma_{\phi N}\,(i\alpha_\phi - 1)}{2}\int\limits_z^\infty \rho(b,y)\,\mathrm{d}y\right]\right|^2. \qquad (14)$$

The general features of the coherent photoproduction are as follows. The t-dependence is given by the elementary $\gamma N \to \phi N$ photoproduction amplitude as well as by the nuclear form factor. The differential cross-section has a diffractive structure due to the $J_0(q_t b)$-dependence. However, up to now this structure was not observed experimentally, since it is non-trivial to isolate coherent from incoherent photoproduction, which dominates at large $|t|$. The forward coherent $\gamma A \to \phi A$ photoproduction cross-section might be used for the extraction of the elementary forward $\gamma N \to \phi N$ cross-section, which can be compared with those collected in fig. 1. The A-dependence of coherent photoproduction allows one to extract $\sigma_{\phi N}$ only under certain constraints on α_ϕ. That extraction is independent of the VDM assumptions.

Indeed if the distortion of the ϕ-meson is negligible and $q_l = 0$ the coherent photoproduction cross-section is proportional to A^2 as is given by eq. (14). Furthermore, to analyze the Cornell data and for completeness, we specified the density distribution function $\rho(r)$ used in eq. (14) as

$$\rho(r) = \frac{\rho_0}{1 + \exp[(r-R)/d]}, \qquad (15)$$

with parameters

$$R = 1.28A^{1/3} - 0.76 + 0.8A^{-1/3}\,\mathrm{fm}, \quad d = \sqrt{3}/\pi\,\mathrm{fm}, \qquad (16)$$

for the nuclei with $A > 16$. For light nuclei we adopt [58,59]

$$\rho(r) = (R\sqrt{\pi})^{-3}\left[4 + \frac{2(A-4)r^2}{3R^2}\right]\exp[-r^2/R^2], \qquad (17)$$

with $R = \sqrt{2.5}$ fm.

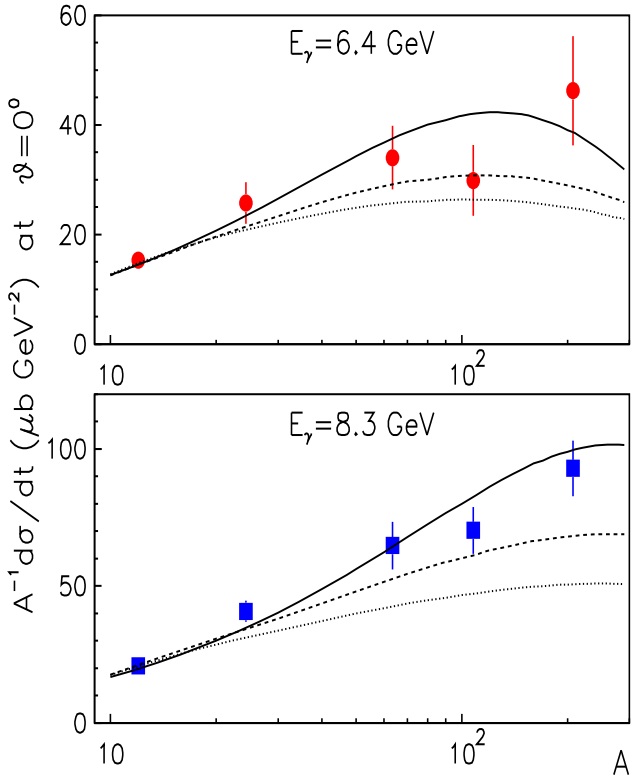

Fig. 5. The forward $\gamma A \to \phi A$ differential cross-section as a function of the mass number. The symbols show the data collected at Cornell [22] at photon energies 6.4 (circles) and 8.3 GeV (squares). The lines are the calculations with the total ϕN cross-section of 10 (solid), 30 (dashed) and 50 mb (dotted) and with the ratio $\alpha_\phi = 0$. Both experimental results and calculations are divided by A. The calculations are normalized at the $A = 12$ point.

We note that the results on forward photoproduction are not sensitive to the variation of the ratio α_ϕ, as can be seen from eq. (14) and is known from the analyses of ρ-meson photoproduction [24] and hadronic elastic scattering [57].

Finally, the lines in fig. 4 are the calculations based on eq. (14) with momentum $q_l = 82$ (dotted line) and 63 (dashed line) and 0 MeV/c (solid line), related to the photon energy by eq. (12). The results are shown as a function of the total ϕN cross-section. The calculations for $q_l = 0$ MeV/c correspond to the high-energy limit, *i.e.* $k \gg m_\phi$, and for $\sigma_{\phi N} = 0$ actually match the A^2 point. To get the slope α we fit our calculation with the function cA^α with c as a constant and using the set of nuclear targets corresponding to the experimentals. Figure 4 illustrates that the q_l correction already introduces a substantial departure from the A^2-dependence. Although the uncertainties in the $\sigma_{\phi N}$ extraction from the data are large, the data are in very good agreement with the calculations with a total ϕN cross-section $\simeq 10$ mb.

Figure 5 shows the forward $\gamma A \to \phi A$ differential cross-section as a function of the target mass number A. The circles and squares are the experimental results obtained at Cornell for photon energies of 6.4 and 8.3 GeV, respectively. The lines show the calculations for different $\sigma_{\phi N}$ and for the ratio $\alpha_\phi = 0$. Both data and calculations are divided[5] by A. Obviously, the shape of the A-dependence is different for the calculation for the various $\sigma_{\phi N}$. The experimental results are in perfect agreement with the calculations using $\sigma_{\phi N} = 10$ mb.

Finally, one can as well extract the elementary $\gamma N \to \phi N$ forward differential cross-section using eq. (14) and compare the results with the results obtained by direct measurement. The calculations with $\sigma_{\phi N} = 10$ mb can be well fitted to the data with an elementary $\gamma N \to \phi N$ forward differential cross-section around 2.2–2.6 μb/GeV^2, which is in good agreement with the results collected in fig. 1.

3.2 Incoherent photoproduction

Recently incoherent ϕ-meson photoproduction at photon energies $1.5 \le E_\gamma \le 2.4$ GeV was studied by the SPRING-8 Collaboration [20]. The data were published with arbitrary normalization and provide the A-dependence fitted by the function A^α with slope $\alpha = 0.72 \pm 0.07$.

The optical model expression for the incoherent photoproduction including only the excitation of the single nucleon and neglecting the Pauli principle, which suppresses the cross-section at small t, is given by [24]

$$\frac{\mathrm{d}\sigma^{inc}_{\gamma A\to\phi A}}{\mathrm{d}t} = \frac{\mathrm{d}\sigma_{\gamma N\to\phi N}}{\mathrm{d}t} \int_0^\infty \mathrm{d}^2 b \int_{-\infty}^{\infty} \mathrm{d}z\, \rho(b,z) \times \exp\left[-\sigma_{\phi N} \int_z^\infty \rho(b,y)\,\mathrm{d}y\right]. \quad (18)$$

Now if $\sigma_{\phi N} = 0$, the forward cross-section is proportional to A. The shaded box in fig. 6 shows the result from SPRING-8, while the line indicates the calculations based on eq. (18) for different values of the total ϕN cross-section. Again, we fit our results by the function cA^α and use the set of nuclear targets from experiment[6]. It is clear that the experimental results favor $23 \le \sigma_{\phi N} \le 63$ mb. This is in agreement with the experimental finding [20] given as $\sigma_{\phi N} = 35^{+17}_{-11}$ mb. The Pauli-blocking corrections make almost no change to the A-dependence and only suppress the absolute value of the forward photoproduction cross-section [24,60].

[5] Although in view of eq. (14) it is more natural to divide the results on coherent photoproduction by A^2, it turns out that the A^{-1} representation is more illustrative in case of the observed moderate A-dependence of the data and therefore is very frequently used.

[6] The A^α-function is not the dependence given by eq. (18) and only provides a useful representation of the data. Indeed the slope α depends on the set of target numbers A used in the calculations. Therefore it is necessary to simulate the experimental conditions explicitely.

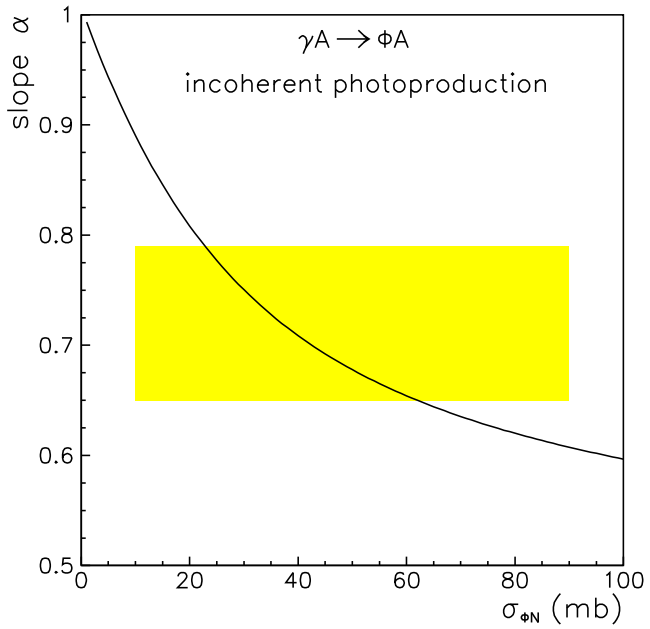

Fig. 6. The slope α of the A^{α}-dependence of the incoherent ϕ-meson photoproduction cross-section as a function of the total ϕN cross-section. The shaded boxes indicate the results at photon energies $1.5 \leq E_{\gamma} \leq 2.4$ GeV obtained by SPRING-8 [20]. The lines show the calculations by eq. (18).

Clearly, this result differs substantially from the total ϕN cross-section extracted from coherent ϕ-meson photoproduction. There are no available explanations why the distortion of the incoherently produced ϕ-meson is so extremely strong. Furthermore, the calculations [60,61] wich include the in-medium modification of the ϕ-meson cannot account for such strong distortion.

4 Coupled-channel scattering

Since ϕ and ω mesons have the same quantum numbers, these two states should mix with each other —see, *e.g.*, [62–64]. Therefore the ϕ-meson might be produced indirectly, *i.e.* through the photoproduction of the ω-meson followed by the $\omega \to \phi$ transition. Furthermore, there can in principle occur an arbitrary number of $\omega \leftrightarrow \phi$ transitions. Moreover, these transitions can occur either due to the ω and ϕ mixing, *i.e.* similar to oscillations, or because of the $\omega N \to \phi N$ interaction. This is illustrated in fig. 7. Since both ω and ϕ mesons are strongly interacting particles, their final-state interaction in any nuclear target would cause distortions.

The coupled-channel scattering apparently depends on the strength of the $\omega \leftrightarrow \phi$ transition. However, one expects the ϕ-meson distortion to be considerable because of the interference effect. Even a small amount of an ω-ϕ admixture might have a considerable effect on ϕ-meson production from complex nuclei. First discussed by Ross and Stodolsky [53,62], this effect has subsequently been largely overlooked in the literature [24]. Here, we consider

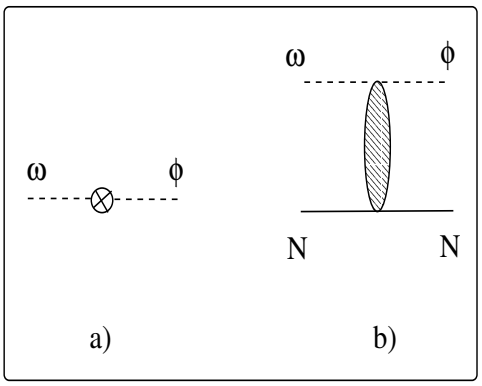

Fig. 7. Mechanisms of $\omega \to \phi$ conversion: a) direct ω-ϕ mixing amplitude and b) the $\omega N \to \phi N$ interaction, where N denotes a nucleon. Type b) contains the direct mechanism a) besides other effects.

coherent and incoherent ϕ-meson photoproduction from nuclei within the coupled-channel approach.

4.1 Coherent photoproduction

The generalization of the single-channel amplitude of for the two coupled-channel scattering can be done by introducing the 2×2 matrix instead of the last term of eq. (11) as

$$\begin{pmatrix} 1-\frac{\sigma_{\omega N}}{2}\int\limits_z^{\infty}\rho(b,y)\mathrm{d}y, & \frac{-\Sigma_{\omega\phi}}{2}\int\limits_z^{\infty}\exp[i\tilde{q}_l y]\rho(b,y)\mathrm{d}y, \\ \frac{-\Sigma_{\omega\phi}}{2}\int\limits_z^{\infty}\exp[-i\tilde{q}_l y]\rho(b,y)\mathrm{d}y, & 1-\frac{\sigma_{\phi N}}{2}\int\limits_z^{\infty}\rho(b,y)\mathrm{d}y, \end{pmatrix} \quad (19)$$

where we have used eqs. (4), (13) and we denote by Σ the effective $\omega \to \phi$ and $\phi \to \omega$ transition cross-sections, which are equivalent because of time-reversal invariance. Furthermore, we neglect the real parts of the elastic and transition amplitudes, since even in the single-channel analysis they could not be fixed. Furthermore, the longitudinal momentum $\tilde{q}_l$ is defined as

$$\tilde{q}_l \simeq \frac{m_{\phi}^2 - m_{\omega}^2}{2k} \ . \quad (20)$$

Neglecting the off-diagonal transition, *i.e.* setting $\Sigma = 0$, the matrix of eq. (19) allows one to recover the single-channel optical model for ω- and ϕ-meson photoproduction, while taking the elementary $\mathcal{T}_{\gamma N}$ amplitude as a two-component vector.

Since in our case Σ is small, the amplitude for coherent ϕ-meson photoproduction from a nucleus can be expressed

in a simple form,

$$\mathcal{T}^{coh}_{\gamma A\to\phi A} = \int_0^\infty \mathrm{d}^2b\; J_0(q_t b) \int_{-\infty}^{\infty} \mathrm{d}z\, \rho(b,z)\, \exp[iq_l z]$$
$$\times \left(\mathcal{T}_{\gamma N\to\omega N} \frac{-\Sigma \int_z^\infty \exp[i\tilde{q}_l y]\, \rho(b,y)\mathrm{d}y}{(\sigma_{\phi N} - \sigma_{\omega N}) \int_z^\infty \rho(b,y)\mathrm{d}y} \right.$$
$$\times \left[\exp\left[-\frac{\sigma_{\omega N}}{2} \int_z^\infty \rho(b,y)\mathrm{d}y \right] - \exp\left[-\frac{\sigma_{\phi N}}{2} \int_z^\infty \rho(b,y)\mathrm{d}y \right] \right]$$
$$\left. + \mathcal{T}_{\gamma N\to\phi N} \exp\left[-\frac{\sigma_{\phi N}}{2} \int_z^\infty \rho(b,y)\mathrm{d}y \right] \right). \qquad (21)$$

For $\Sigma = 0$, eq. (21) reduces to eq. (11) and the coherent differential cross-section is given by eq. (14). Moreover, eq. (21) corresponds to the first-order perturbation expansion in Σ, *i.e.* the inclusion of only one $\omega \to \phi$ transition. If Σ is large one should consider an arbitrary number of $\omega \leftrightarrow \phi$ transitions, which might be done through the series expansion [65] of the off-diagonal elements of the matrix given by eq. (19).

Moreover, in high-energy limit, *i.e.* when $q_l = \tilde{q}_l = 0$, the integration along z can be done analytically and the coherent photoproduction amplitude is then given in a well-known form [51]

$$\mathcal{T}^{coh}_{\gamma A\to\phi A} = \int_0^\infty \mathrm{d}^2b\; J_0(q_t b) \left[\frac{\mathcal{T}_{\gamma N\to\omega N}\; \Sigma}{\sigma_{\omega N} - \sigma_{\phi N}} \right.$$
$$\times \left(\frac{1 - \exp\left[-\frac{\sigma_{\omega N}\, T(b)}{2} \right]}{\sigma_{\omega N}} - \frac{1 - \exp\left[-\frac{\sigma_{\phi N}\, T(b)}{2} \right]}{\sigma_{\phi N}} \right)$$
$$\left. + \frac{\mathcal{T}_{\gamma N\to\phi N}}{\sigma_{\phi N}} \left(1 - \exp\left[-\frac{\sigma_{\phi N}\, T(b)}{2} \right] \right) \right], \qquad (22)$$

where the real parts of the scattering amplitudes were neglected and the thickness function is given as

$$T(b) = \int_{-\infty}^{\infty} \rho(b,z)\, \mathrm{d}z. \qquad (23)$$

Following the VDM results shown in figs. 1, 3 we use the elementary elastic ω- and ϕ-meson photoproduction amplitude given by eq. (7), namely as

$$\mathcal{T}_{\gamma N\to VN} = \frac{\sqrt{\alpha}}{4\gamma_V} \frac{q_V}{q_\gamma} \sigma_{VN}, \qquad (24)$$

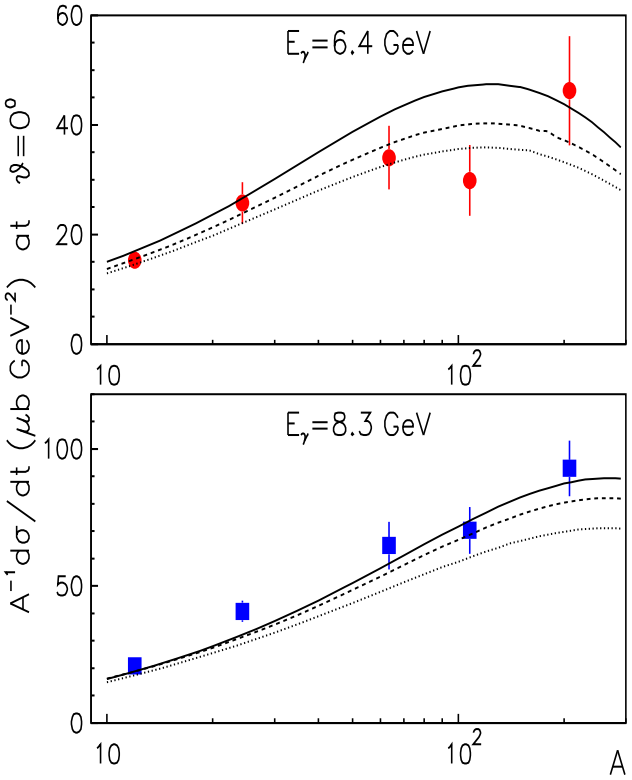

Fig. 8. The forward $\gamma A \to \phi A$ differential cross-section as a function of the mass number. The symbols show the data collected at Cornell [22] at photon energies 6.4 (circles) and 8.3 GeV (squares). The lines are the coupled-channel scattering calculations by eq. (21) with the total ϕN cross-section of 11 mb and the ωN cross-section of 23 mb and for the transition $\Sigma = 0$ (solid), 0.3 (dashed) and 0.5 mb (dotted). Both experimental results and calculations are divided by A. The normalization of the calculations is fixed by VDM as explained in the text.

with the γ_ϕ and γ_ω coupling constants given by eq. (3) and with $\sigma_{\phi N} = 11$ mb and $\sigma_{\omega N} = 23$ mb. Thus, the absolute normalization of our calculations is fixed by VDM. Figure 8 shows the coherent $\gamma A \to \phi A$ differential cross-section as a function of the mass number calculated for different values of Σ. The data [22] might be well reproduced by calculations with $0 \le \Sigma \le 0.3$ mb. Only the experimental results at $E_\gamma = 6.4$ GeV support the coupled-channel effect originating from the $\omega \to \phi$ transition.

4.2 Incoherent photoproduction

Let us now consider incoherent photoproduction of ω-mesons followed by $\omega N \to \phi N$ scattering. Note that in the coupled-channel description of coherent ϕ-meson photoproduction the $\omega \to \phi$ transition is not necessaryly due to the scattering on the target nucleon, but might be also an oscillation due to the mixing. In that sense incoherent photoproduction is given as a two-step process and the

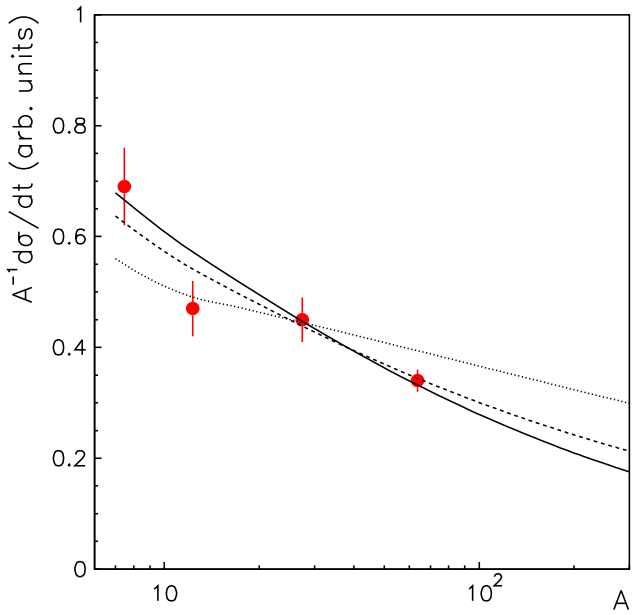

Fig. 9. The incoherent ϕ-meson photoproduction cross-section as a function of the mass number. The circles show the data collected at SPRING-8 [20]. The solid line is the coupled-channel scattering calculations by eq. (25) with the total ϕN cross-section of 11 mb and the ωN cross-section of 23 mb, while the dashed line is the result obtained with $\sigma_{\phi N} = 11$ mb and $\sigma_{\omega N} = 30$ mb. The dotted line is the single-channel results for $\sigma_{\phi N} = 11$ mb. Both experimental results and calculations are divided by A. The normalization of the calculations is fixed at the Al target.

differential cross-section can be written as [48,66,67]

$$\frac{\mathrm{d}\sigma^{inc}_{\gamma A\to\phi A}}{\mathrm{d}t} = \frac{\mathrm{d}\sigma_{\gamma N\to\omega N}}{\mathrm{d}t}\int\limits_0^\infty \tilde{\Sigma}\mathrm{d}^2b\left[\frac{1-\exp[-\sigma_{\phi N}\,T(b)]}{\sigma_{\phi N}} - \frac{\exp[-\sigma_{\omega N}\,T(b)]-\exp[-\sigma_{\phi N}\,T(b)]}{\sigma_{\phi N}-\sigma_{\omega N}}\right], \quad (25)$$

where the function $T(b)$ is given by eq. (23) and it is not necessary that $\Sigma = \tilde{\Sigma}$. Considering both the direct and the two-step ϕ-meson production, one should in principle add the contribution given by eq. (18).

Unfortunately, the data [20] on incoherent ϕ-meson photoproduction from nuclei are given with arbitrary normalization and we cannot investigate how big the possible contribution from two-step production might be, since $\tilde{\Sigma}$ is unknown. However, it is possible to examine the A-dependence due to the two-step process.

Figure 9 shows the incoherent ϕ-meson photoproduction cross-section as a function of the target mass measured at SPRING-8 [20]. The dotted line shows the calculations performed within the single-channel optical model using eq. (18) with $\sigma_{\phi N} = 11$ mb. The solid line represents the result obtained with the coupled-channel model calculation, eq. (25), using $\sigma_{\phi N} = 11$ mb and $\sigma_{\omega N} = 23$ mb. Both the data and our results are divided by A. The calculations are normalized for an Al target. The single-channel calculations are identical to the ones shown in refs. [20, 60,61] and apparently cannot reproduce the data, as we already discussed in sect. 3.2. The two-step model calculations are in reasonable agreement with experimental results —providing an A-dependence $\propto A^{0.63}$. Thus, the measured A-dependence clearly indicates the dominance of the two-step process in ϕ-meson photoproduction. Unfortunately, there are no data available for heavy targets, which clearly are crucial for the verification of the calculated A-dependence shown in fig. 9.

Note that another two-step process, *i.e.* $\gamma N \to \pi N$ followed by the $\pi N \to \phi N$ transition, would produce almost the same dependence, $\propto A^{0.63}$, as shown by the dashed line in fig. 9. In the considered π-meson momentum range the total πN cross-section is about $\simeq 30$ mb and therefore calculations were done using eq. (25) with $\sigma_{\omega N} = 30$ mb. Note that both π-meson photoproduction and the $\pi N \to \phi N$ transition are quite large and therefore it is possible that incoherent ϕ-meson photoproduction is dominated by a two-step reaction mechanism. For instance, theoretical studies [68–72] on low-energy K^+, ρ, ω and ϕ-meson production in proton nucleus collisions indicate the dominance of the two-step process with intermediate π-mesons. This result is strongly supported by measurements of the A-dependence and two-particle correlations in K^+-meson production from pA reactions [70, 73–76]. Further investigations on incoherent ϕ-meson photoproduction require measurement of differential cross-section with absolute normalization.

It is also clear that incoherent coupled-channel ϕ-meson photoproduction might also proceed through coherent ω-meson production by the photon, followed by the incoherent $\omega \to \phi$ transition. This mechanism involves, in addition, substantial q_l-dependence at low photon energies similar to that of eq. (14), which allows for freedom in the description of the A-dependence.

4.3 Estimates for Σ and $\tilde{\Sigma}$

It is useful to estimate the Σ and $\tilde{\Sigma}$ in order to understand how large the effect due to the $\omega \to \phi$ transition might be. Our estimates are based on the amplitudes evaluated in free space, which are not necessarily the same as in nuclear matter.

Very recently the ω-ϕ mixing amplitude $\Theta_{\omega\phi}$ was investigated [77] within the leading-order chiral perturbation theory and it was found that $\Theta_{\omega\phi} = (25.34 \pm 2.39) \times 10^{-3}$ GeV^2. In our normalization Σ can be related to $\Theta_{\omega\phi}$ as [78]

$$\Sigma \simeq \frac{1}{m_\omega^2}\frac{\Theta^2_{\omega\phi}}{(m_\phi^2 - m_\omega^2)^2} = 2.2\ \mu\mathrm{b}, \quad (26)$$

where we neglect the width of the ω- and ϕ-meson. Actually, the effect due to the ω-ϕ mixing is small and as is indicated by the calculations shown in fig. 8 might be supported by the Cornell data [22] on coherent ϕ-meson photoproduction from nuclei. However, the data itself do

not really require the inclusion of the mixing amplitude and the problem still remains open.

The contribution to incoherent ϕ-meson photoproduction from the two-step process with an intermediate π-meson can be reasonably estimated since there are data available for the $\pi N \to \phi N$ reaction collected in refs. [79, 80] and parameterized as

$$\tilde{\Sigma}(\pi N \to \phi N) = \frac{18\sqrt{s - s_0}}{0.1285 + (s - s_0)^2} \quad \mu\text{b}, \tag{27}$$

where s is the squared invariant mass of the πN system given in GeV^2 and $\sqrt{s_0} = m_N + m_\phi$ is the reaction threshold. Note that at pion energies $\simeq 2$ GeV, which correspond to the forward ϕ-meson photoproduction in the SPRING-8 experiment [20] the $\pi N \to \phi N$ cross-section is about 20 μb. Furthermore, at photon energies $1.5 \leq E_\gamma \leq 2.4$ GeV the total cross-section for the $\gamma N \to \phi N$ reaction is on average $\simeq 0.3\,\mu$b [81], while the $\gamma N \to \pi N$ reaction accounts for $\simeq 1\,\mu$b [82,83]. Therefore the contribution from the two-step mechanism might be well suppressed as compared to the direct ϕ-meson photoproduction. This can be clearly seen by inspecting eqs. (18), (25) and replacing the ωN intermediate state with the πN one.

It is difficult to estimate reliably the contribution to incoherent ϕ-meson photoproduction from a two-step process with an intermediate ω-meson. Figures 2, 3 illustrate that the incoherent forward ω-meson photoproduction dominates the ϕ-meson photoproduction by a factor of order $\simeq 60$. However, at the same time the $\gamma p \to \phi p$ data collected in fig. 3 show almost no room for the non-diagonal $\omega N \to \phi N$ transition. The data at low photon energies are well described by the VDM accounting only for elastic diagonal $\phi N \to \phi N$ scattering. Within the experimental uncertainties of the forward $\gamma p \to \phi p$ differential cross-sections and considering the difference between data and our VDM calculations with $\sigma_{\phi N} = 11$ mb we estimate $\tilde{\Sigma} < 0.1$ mb. In that case the contribution from the two-step process is compatible with the direct incoherent ϕ-meson photoproduction and the coupled-channel effect is indeed sizable.

4.4 Speculations

Finally, we would like to mention another possibility which is not related to the ϕ-meson propagation in nuclear matter and the $\tilde{\Sigma}$ transition but with incoherent ϕ-meson photoproduction at low energies. Recently [84], we investigated the role of the cryptoexotic baryon with hidden strangeness, $B_\phi = uudds\bar{s}$, in ϕ-meson production in proton-proton collisions close to the reaction threshold. We found that the enhanced ϕ-meson production observed at COSY [21] can be well explained by an B_ϕ-baryon excitation followed by the $B_\phi \to \phi N$ decay. It is expected that these pentaquark baryons have a narrow width and decay preferentially into the ϕN, $K\bar{K}N$ or YK channels, where Y stands for ground-state or excited hyperons [85,86]. Experimental observations for the B_ϕ candidates were reported in refs. [87–92]. The high-statistics study of ref. [92] of the $\Sigma^0 K^+$ mass spectrum indicates two exotic states with $M = 1807 \pm 7$ MeV, $\Gamma = 62 \pm 19$ MeV and $M = 1986 \pm 6$ MeV, $\Gamma = 91 \pm 20$ MeV.

One might expect that B_ϕ-baryon can be excited in photon-nucleon interaction. Because of its mass the $\gamma p \to \phi p$ reaction would be sensitive to B_ϕ excitation at low photon energy. The B_ϕ contribution might explain the SAPHIR-8 and SPRING-8 measurements [40,41] of angular spectra in the Gottfried-Jackson frame, which indicate that at low energies the ϕ-meson photoproduction is not governed by pomeron exchange.

Considering the coherent and incoherent ϕ-meson photoproduction from nuclei we notice even more significant features. First, the coherent photoproduction at low energies should not by dominated by B_ϕ-baryon excitation, since in that case the residual nucleus differs from ground state. The incoherent ϕ-meson photoproduction at low energies might be dominated by B_ϕ excitation. Since the B_ϕ-baryon is narrow, it decays outside the nucleus and an effective distortion of the ϕ-meson is given by the distortion of B_ϕ, which is similar to an interaction of other baryons in nuclear matter because of the light quark content of the B_ϕ-baryon. Therefore one should not be surprised by the result shown in fig. 6.

5 Conclusions

We have analyzed the coherent and incoherent ϕ-meson photoproduction from nuclei by applying the single- and coupled-channel optical model.

The data on the coherent ϕ-meson photoproduction collected at Cornell [22] at photon energies of 6.4 and 8.3 GeV can be well reproduced by a single-channel calculation taking into account the ϕ-meson distortion compatible with the ϕN total cross-section $\sigma_{\phi N} = 10$ mb. This result is in good agreement with the VDM analysis of the forward $\gamma p \to \phi p$ differential cross-section, which indicates that $\sigma_{\phi N} \simeq 11$ mb. The coherent ϕ-meson photoproduction shows little room for the coupled-channel effect due to the contribution from the $\omega \to \phi$ transition.

The data on the incoherent ϕ-meson photoproduction off various nuclei collected at SPRING-8 [20] at photon energies from 1.5 to 2.4 GeV can be reproduced by the single-channel optical model calculations only under the assumption that the ϕ-meson is substantially distorted in nuclei, which corresponds to $23 \leq \sigma_{\phi N} \leq 63$ mb. This result is in agreement with previous incoherent ϕ-meson photoproduction data analyses [20,60,61]. Moreover, we found that taking into account the coupled-channel effects, *i.e.* assuming direct ω-meson photoproduction followed by the $\omega N \to \phi N$ transition as well as pion photoproduction followed by the $\pi N \to \phi N$ scattering, it is possible to reproduce the A-dependence measured at SPRING-8 [20].

Although we estimate the absolute rates for the contribution of these two different intermediate states, it is difficult to draw a final conclusion. First, the SPRING-8 data [20] are published without absolute normalization. Second, the t-dependence of these data are not given for all nuclei used in the measurements. Such knowledge is

essential for the evaluation of incoherent photoproduction within the coupled-channel analysis, since each of the two-step processes has an individual t-dependence, which can be used in order to distinguish the intermediate states. In that sense more precise data on incoherent ϕ-meson photoproduction are necessary for further progress.

We also discussed a very alternative (and probably speculative) scenario that might occur only in incoherent ϕ-meson photoproduction but is not accessible in the coherent reaction. The excitation of the cryptoexotic baryon with hidden strangeness, called B_ϕ, would result in an A-dependence similar to that measured by SPRING-8 [20]. However, the B_ϕ-baryon could not be exited in coherent photoproduction. Therefore measurements of the A-dependence of coherent ϕ-meson photoproduction from nuclei at low energies are crucial for the identification of the possible existence of such an cryptoexotic baryon.

We would like to thank J. Haidenbauer, T. Nakano, A. Nogga for useful discussions. This work was partially supported by Deutsche Forschungsgemeinschaft through funds provided to the SFB/TR 16 "Subnuclear Structure of Matter". This research is part of the EU Integrated Infrastructure Initiative Hadron Physics Project under contract number RII3-CT-2004-506078. A.S. acknowledges support by the JLab grant SURA-06-C0452 and the COSY FFE grant No. 41760632 (COSY-085).

References

1. T. Hatsuda, T. Kunihiro, Phys. Lett. B **185**, 304 (1987).
2. V. Bernard, U.-G. Meißner, I. Zahed, Phys. Rev. Lett. **59**, 966 (1987).
3. V. Bernard, U.-G. Meißner, Nucl. Phys. A **489**, 647 (1988).
4. G.E. Brown, M. Rho, Phys. Rev. Lett. **66**, 2720 (1991).
5. T. Hatsuda, S.H. Lee, Phys. Rev. C **46**, 34 (1992).
6. G.Q. Li, C.M. Ko, G.E. Brown, Nucl. Phys. A **606**, 568 (1996) [nucl-th/9608040].
7. K. Saito, K. Tsushima, A.W. Thomas, arXiv:hep-ph/0506314.
8. G. Agakichiev *et al.*. Phys. Rev. Lett. **75**, 1272 (1995).
9. M. Masera *et al.*, Nucl. Phys. A **590**, 93 (1992).
10. G. Agakichiev *et al.*. Phys. Lett. B **422**, 405 (1998).
11. K. Ozawa *et al.*, Phys. Rev. Lett. **86**, 5019 (2001) [nucl-ex/0011013].
12. D. Trnka *et al.*, Phys. Rev. Lett. **94**, 192303 (2005) [nucl-ex/0504010].
13. M. Naruki *et al.*, Phys. Rev. Lett. **96**, 092301 (2006) [nucl-ex/0504016].
14. R. Muto *et al.*, nucl-ex/0511019.
15. T. Tabaru *et al.*, nucl-ex/0603013.
16. G.J. Lolos, AIP Conf. Proc. **814**, 608 (2006).
17. W. Lenz, Z. Phys. **56**, 778 (1929).
18. C.D. Dover, J. Hüfner, R.H. Lemmer, Ann. Phys. **66**, 248 (1971).
19. B. Friman, Acta Phys. Pol. B **29**, 3195 (1998) [nucl-th/9808071].
20. T. Ishikawa *et al.*, Phys. Lett. B **608**, 215 (2005) [nucl-ex/0411016].
21. M. Hartmann *et al.*, Phys. Rev. Lett. **96**, 242301 (2006) [hep-ex/0604010].
22. G. McClellan *et al.*, Phys. Rev. Lett. **26**, 1593 (1971).
23. L. Stodolsky, Phys. Rev. Lett. **18**, 135 (1967).
24. T.H. Bauer, R.D. Spital, D.R. Yennie, F.M. Pipkin, Rev. Mod. Phys. **50**, 261 (1978).
25. E. Paul, Nucl. Phys. A **446**, 203 (1985).
26. Y. Nambu, J.J. Sakurai, Phys. Rev. Lett. **8**, 79 (1962).
27. Particle Data Group, Phys. Lett. B **592**, 1 (2004).
28. J. Hufner, B.Z. Kopeliovich, Phys. Lett. B **426**, 154 (1998) [hep-ph/9712297].
29. A. Sibirtsev, K. Tsushima, A.W. Thomas, Phys. Rev. C **63** 044906 (2001) [nucl-th/0005041].
30. A. Sibirtsev, S. Krewald, A.W. Thomas, J. Phys. G **30**, 1427 (2004) [nucl-th/0301082].
31. H. Alvensleben *et al.*, Phys. Rev. Lett. **27**, 444 (1971).
32. R. Erbe *et al.*, Phys. Rev. **175**, 1669 (1968).
33. J. Ballam *et al.*, Phys. Rev. D **7**, 3150 (1973).
34. H.J. Besch *et al.*, Nucl. Phys. B **70**, 257 (1974).
35. H.J. Behrend *et al.*, Phys. Lett. B **56**, 408 (1975).
36. D.P. Barber *et al.*, Phys. Lett. B **79**, 150 (1978).
37. M. Atkinson *et al.*, Z. Phys. C **27**, 233 (1985).
38. J. Busenitz *et al.*, Phys. Rev. D **40**, 1 (1989).
39. M. Derrick *et al.* Phys. Lett. B **377**, 259 (1996).
40. J. Barth *et al.*, Eur. Phys. J. A **17**, 269 (2003).
41. T. Mibe *et al.*, Phys. Rev. Lett. **95**, 182001 (2005) [nucl-ex/0506015].
42. A. Sibirtsev, K. Tsushima, S. Krewald, Phys. Rev. C **67**, 055201 (2003) [nucl-th/0301015].
43. B. Friman, M. Soyeur, Nucl. Phys. A **600**, 477 (1996) [nucl-th/9601028].
44. S.M. Berman, S.D. Drell, Phys. Rev. B **133**, 791 (1964).
45. A. Sibirtsev, K. Tsushima, S. Krewald, AIP Conf. Proc. **717**, 280 (2004) [nucl-th/0202083].
46. R.J. Glauber, *High Energy Physics and Nuclear Structure*, edited by S. Ddevons (Plenum, New York, 1970) p. 207.
47. D.R. Yennie, *Hadronic Interactions of Electrons and Photons*, edited by J. Cummings, H. Osborn (Academic Press, New York, 1971) p. 321.
48. G.V. Bochman, Phys. Rev. D **6**, 1938 (1972).
49. S.D. Drell, J.S. Trefil, Phys. Rev. Lett. **16**, 552 (1966).
50. B. Margolis, Phys. Lett. **26**, 254 (1968).
51. K.S. Kölbig, B. Margolis, Nucl. Phys. B **6**, 85 (1968).
52. G. McClellan *et al.*, Phys. Rev. Lett. **26**, 1597 (1971).
53. M. Ross, L. Stodolsky, Phys. Rev. **149**, 1172 (1966).
54. J.S. Trefil, Phys. Rev. **180**, 1379 (1969).
55. J.S. Trefil, Nucl. Phys. B **11**, 330 (1969).
56. R.G. Newton, *Scattering Theory of Waves and Particles* (Springer-Verlag, Berlin, 1982) p. 605.
57. A. Sibirtsev, W. Cassing, Phys. Rev. C **61**, 057601 (2000) [nucl-th/9909053].
58. O.D. Dalkarov, V.A. Karmanov, Phys. Lett. B **147**, 1 (1984).
59. G.D. Alkhasov, S.L. Belostotsky, A.A. Vorobyov, Phys. Rep. C **42**, 89 (1978).
60. D. Cabrera, L. Roca, E. Oset, H. Toki, M.J. Vicente Vacas, Nucl. Phys. A **733**, 130 (2004).
61. P. Münlich, U. Mosel, Nucl. Phys. A **765**, 188 (2006) [nucl-th/0510078].
62. M. Ross, L. Stodolsky, Phys. Rev. Lett. **17**, 563 (1966).
63. J.S. Trefil, Nucl. Phys. B **29**, 575 (1971).
64. A.I. Sandra, A. Wijangco, Phys. Rev. D **5**, 661 (1972).

65. O. Benhar, S. Fantoni, N.N. Nikolaev, B.Z. Zakharov, J. Exp. Theor. Phys. **84**, 421 (1997).
66. G. Fäldt, P. Osland, Nucl. Phys. B **87**, 445 (1975).
67. E. Vercellin *et al.*, Nuovo Cimento A **106**, 861 (1992).
68. W. Cassing, G. Batko, U. Mosel, K. Niita, G. Wolf, O. Schult, Phys. Lett. B **238**, 25 (1990).
69. A. Sibirtsev, M. Büscher, Z. Phys. A **347**, 191 (1994).
70. M. Debowski *et al.*, Z. Phys. A **356**, 313 (1996).
71. A. Sibirtsev, W. Cassing, U. Mosel, Z. Phys. A **358**, 357 (1997) [nucl-th/9607047].
72. E.Ya. Paryev, Eur. Phys. J. A **7**, 127 (2000).
73. V.P. Koptev *et al.*, Sov. Phys. JETP **94**, 1 (1988).
74. A. Badala *et al.*, Phys. Rev. Lett. **80**, 4863 (1998).
75. M. Büscher *et al.*, Phys. Rev. C **65**, 014603 (2002) [nucl-ex/0107011].
76. V. Koptev *et al.*, Eur. Phys. J. A **17**, 235 (2003).
77. A. Kucurkaslan, U.-G. Meißner, Mod. Phys. Lett. A **21**, 1423 (2006) [hep-ph/0603061].
78. R. Urech, Phys. Lett. B **355**, 308 (1995) [hep-ph/9504238].
79. A. Sibirtsev, Nucl. Phys. A **604**, 455 (1996).
80. A. Sibirtsev, W. Cassing, Eur. Phys. J. A **7**, 407 (2000).
81. A. Sibirtsev, U.-G. Meißner, A.W. Thomas, Phys. Rev. D **71**, 094011 (2005) [hep-ph/0503276].
82. B.H. Kellett, Nucl. Phys. B **25**, 205 (1970).
83. H. Genzel, P. Joos, W. Pfeil, Landolt-Börnstein, New Ser. **8**, 318 (1973).
84. A. Sibirtsev, J. Haidenbauer, U.-G. Meißner, Eur. Phys. J. A **27**, 263 (2006) [nucl-th/0512055].
85. L.G. Landsperg, Phys. Usp. **37**, 1043 (1994).
86. L.G. Landsperg, Phys. Rep. **320**, 223 (1999).
87. M.W. Arenton *et al.*, Phys. Rev. D **25**, 2241 (1982)
88. A.N. Aleev *et al.*, Z. Phys. C **25**, 205 (1984).
89. V.A. Dorofeev *et al.*, Phys. At. Nucl. **57**, 227 (1994).
90. V.A. Dorofeev *et al.*, Phys. At. Nucl. **57**, 238 (1994).
91. M.Ya. Balatz *et al.*, Z. Phys. C **61**, 223 (1994).
92. Yu.M. Antipov *et al.*, Phys. At. Nucl. **65**, 2070 (2002).